Miniature Antenna for Sensor Network on Human Head

Mohannad Alharbi, Abas Sabouni, *IEEE Member,* and Sima Noghanian, *IEEE Senior Member*

***Abstract*— This paper proposes a novel miniaturized antenna for sensor network with focus on placement on human head. The antenna is within the volume of 3.5x3.5 x1.5 mm^3. It provides directive gain in the direction outward the body.**

I. Introduction

There are various applications such as wireless body area networks [1] and health monitoring systems [1] that require wearable wireless sensors. In such applications multiple antennas are required to be placed in the close vicinity of body. The restriction on size and power requires miniaturization of antennas. Due to restriction on power consumption, antennas should be directive. Some challenges are the losses due to tissue's high conductivity and various loading effects that change antenna's performance in the close proximity of body. In this paper we introduce a novel design that provides directive pattern while it is placed close to human head tissues. The small size of the antenna makes it suitable to be integrated with in an array of sensors place on human head.

II. Design

A. Antenna Design

The main focus in this design was miniaturizing the antenna. Planar Inverted F Antenna (PIFA) on air substrate was chosen first. Various techniques and modifications were applied to optimize the antenna performance when placed on human head. All the simulations were done using commercial simulation program CST Microwave Studio [2]. The proposed antenna is depicted in Fig. 1, and the values of antenna parameters are listed in Table I.

B. Antenna Performance

The antenna was mounted on layers of head tissues as depicted in Fig. 2, as well as a realistic head model as shown in Fig. 3. The realistic model was obtained using three-dimensional (3D) Magnetic Resonance Imaging (MRI) data from a 25 year old healthy human subject. In order to segment the MRI data, we used Statistical Parametric Mapping technique to categorize different regions of the head such as scalp, skull, Cerebro-Spinal Fluid (CSF), Gray Matter (GM), and White Matter (WM). Then the dielectric properties values were assigned to each tissue type. Head tissue dielectric properties were modeled using the second order Debye model as given in (1). These parameters were obtained from [3] except for the CSF parameters that were not provided in [3]. We calculated the average value of CSF dielectric properties at 1 GHz and 10 GHz, obtained from [4], Table II provides the Debye model parameters and Table III presents the calculated average value of CSF.

$$\varepsilon(\omega) = \varepsilon_{\infty} + \sum_{m=1}^{2} \frac{\Delta\varepsilon_m}{1 + j\omega\tau_m} \qquad (1)$$

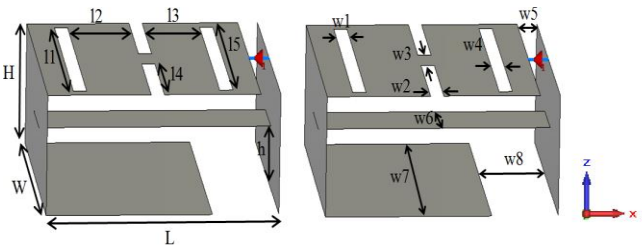

Figure 1. Proposed miniaturized antenna.

TABLE I. Antenna Dimensions.

Parameter	Value (mm)	Parameter	Value (mm)
L	3.50	w1	0.20
W	3.50	w2	0.20
H	1.50	w3	0.50
h	0.75	w4	0.20
l1	3.10	w5	0.30
l2	0.95	w6	0.80
l3	0.85	w7	3.50
l4	1.50	w8	1.00
l5	3.10		

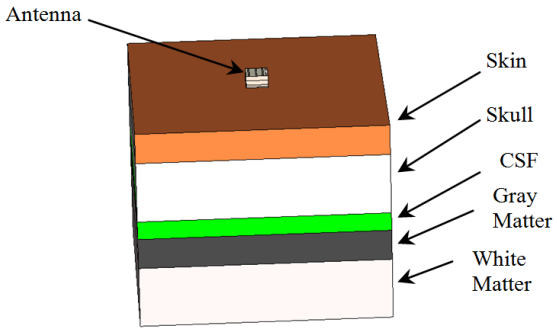

Figure 2. Antenna on a layered model of head tissues.

Resrach supported by Ministry of Higher Education of Saudi Arabia and University of North Dakota.

M. Alharbi is with the Department of Electrical Engineering University of North Dakota, Grand Forks, ND 58202-7165 USA, (email: m.alsati@hotmail.com)

S. Noghanian is with the Department of Electrical Engineering University of North Dakota (corresponding author, phone: 701-777-4433; fax: 701-777-5253; e-mail: sima.noghanian@ engr.und.edu).

A. Sabouni is with the Department of Electrical Engineering, Wilkes University, Wilkes-Barre, PA 18766 USA (email: abas.sabouni@wilkes.edu)

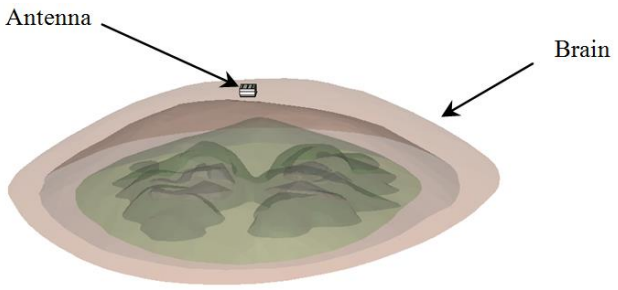

Figure 3. Antenna placed on a realistic head model.

TABLE II. DEBYE PARAMTERS OF HEAD TISSUES [3].

Tissue type	ε_∞	ε_{S1}	ε_{S2}	τ_1 (ps)	τ_2 (ns)	Height (mm)
Skull	4.31	20.43	24.0	10.80	0.46	10
GM	6.37	49.78	85.96	7.52	0.69	5
WM	5.74	36.73	46.48	7.54	0.54	10
Skin	4.39	37.16	70.17	7.42	0.57	5

TABLE III. DIELECTRIC PROPERTIES OF CEREBROSPINAL FLUID (HEIGHT 3MM) [4].

Tissue	Permittivity (ε_r)		Conductivity (σ)		ε_{rave}	σ_{ave}
Frequency (GHz)	*1*	*10*	*1*	*10*	60.40	8.90
CSF	68.40	52.40	2.45	15.37		

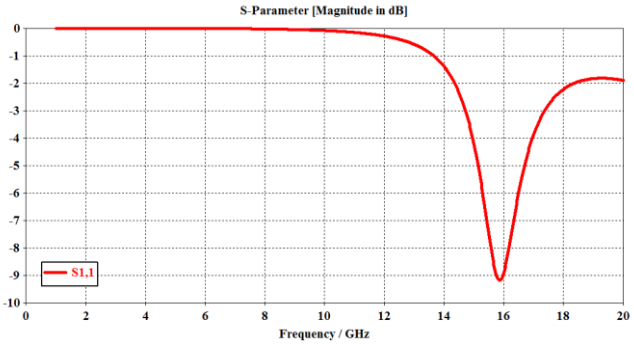

Figure 4. Reflection coefficient of the proposed antenna in free-space.

III. METHODOLOGY AND RESULTS

A. Antenna Performance in Free-Space

In order to study the effect of head tissues on the antenna we first observed the antenna performance in free-space. Figs. 4-7 show the reflection coefficient, the current density, and the radiation patterns of the antenna in free-space, respectively. The antenna resonates at 15.88 GHz. Fig. 5 shows that the current density is mostly on the strip in the middle of the antenna. The antenna is linearly polarized. Co-polarized field components are E_θ on ϕ=0° (E-plane) and E_φ on ϕ=90° plane (H-plane). Since the cross-polarization level is very low the total gain has been shown in Figs. 6-7 and the cross-polarized fields are not separated from co-polarized fields.

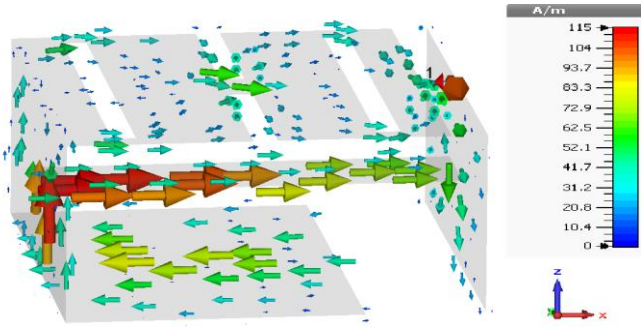

Figure 5. Current density when the antenna is in free-space.

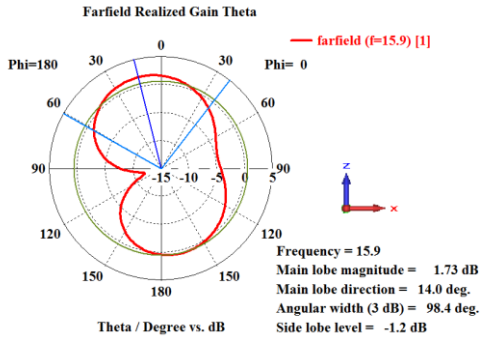

Figure 6. E-plane gain pattern in free-space.

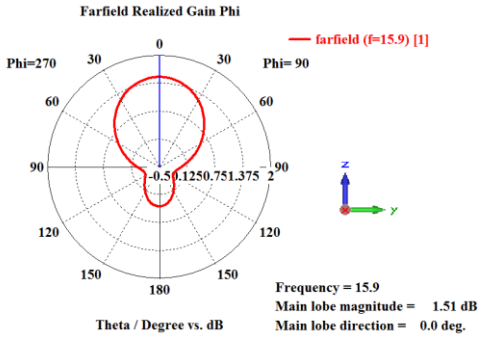

Figure 7. H- plane gain pattern in free-space.

B. Antenna Performance when Placed on Head

The antenna was simulated on a model of head tissue layers. Three surface areas were chosen. Fig. 8 depicts these models with the surface areas of 2x2 cm^2, 4x4 cm^2, and 6x6 cm^2. The simulations were also done when the antenna was placed on the MRI driven segmented head model. It is known that the head tissues have significant loading impact on the antenna's performance, therefore, it was necessary to estimate these effects using a less computational layer models. One major question was how big of the surface area in a layered model was necessary to include the most significant loading effects in the simulation. This could help to make a decision on the size that is needed from segmented head model to have an accurate simulation.

By comparing Figs. 4 and 9 it can be observed that the resonance frequency has shifted from 15.88 GHz (in free-space) to 4.06 GHz on head models. The shift in resonance

frequency, as explained in [5], is due to skin's high permittivity in the vicinity of the antenna. In such situations skin becomes a part of antenna and increases the effect permittivity of the substrate. Thus, the resonance frequency is shifted to a lower value. It is clear from Fig. 9 that the surface area and the head model did not cause any difference in the reduction of frequency, as all cases show the same resonance frequency at 4.06 GHz.

The radiation patterns, however, are very much affected by the surface area. The radiation patterns of four cases are presented in Figs. 10 and 11, and the changes in gain levels are highlighted in Table IV. Co-polarized components are G_θ (ϕ=0) (E-plane) and G_ϕ (ϕ=90°) (H-plane). As stated in Table IV, the gain drops significantly due to tissue losses. The radiation patterns also become more directive in E-plane, as the surface area is increased to 4x4 cm^2. Consequently, we concluded that 4x4 cm^2 of the surface area would be sufficient to include the loading effects.

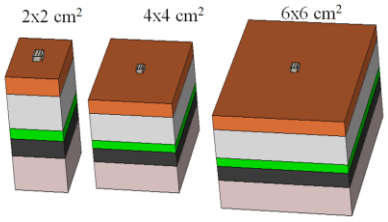

Figure 8. Antenna placed on layered model with three surface areas.

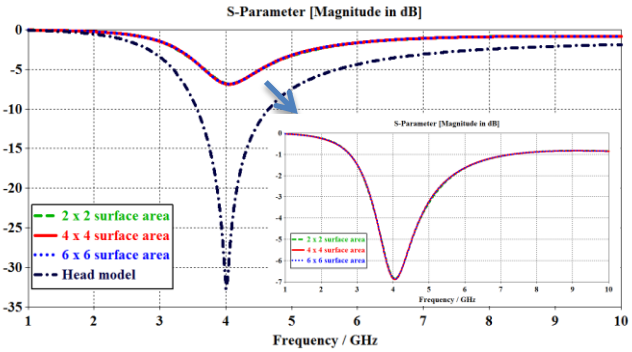

Figure 9. Return loss of antenna on three layered and realstic models.

TABLE IV. ANTENNA GAIN IN DIFFERENT PLANES (DBI).

Case	G_θ (ϕ=0)	$G\varphi$ (ϕ=0)	G_θ (ϕ=90)	$G\varphi$ (ϕ=90)
Free-space	1.7	-107.0	-8.5	1.5
2x2 cm^2	-17.5	-137.0	-35.1	-17.6
4x4 cm^2	-17.9	-134.0	-37.3	-18.0
6x6 cm^2	-16.2	-136.0	-37.4	-16.3
Head model	-16.2	-44.4	-34.2	-16.2

TABLE V. S_{11} AND INPUT IMPEDANCE OF ANTENNA IN FREE-SPACE AND ON 4X4 CM^2 SURFACE AREA.

Case	Frequency GHz	S_{11}(dB)	Real Z_{in} (Ω)	Imag. Z_{in} (Ω)
Free-space	15.90	-9.14	78.83	-36.79
4x4 cm^2	4.06	-6.86	32.8	37.5

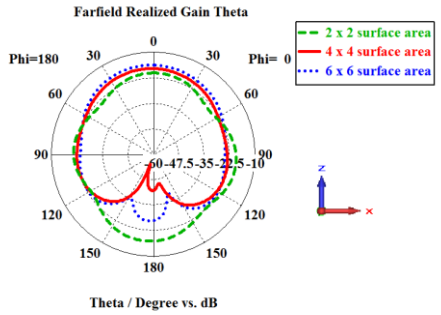

Figure 10. E-plane gain patterns on tissue layers.

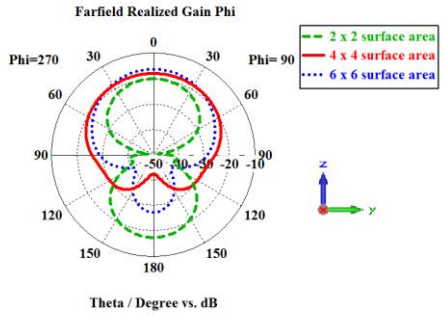

Figure 11. H-plane gain patterns on tissue layers.

C. *Antenna Performance Enhancement*

Since the gain is very low, further performance enhancement is needed. Two techniques were performed to improve the performance of the antenna. First, the reflection coefficient of the antenna was enhanced by replacing the air substrate with a high dielectric layer. The chosen substrate was Alumina (99.5%) (ε_r=9.9, tanδ=0.0001). The reflection coefficient of the antenna after addition of Alumina substrate for the case that antenna is placed on a layer model with 4x4 cm^2 is depicted in Fig. 12. The resonance frequency dropped from 4.06 GHz to 3.80 GHz. However, there was no change in the gain due to skin layer loading effects (Case 1 in Figs. 12-14). To improve the gain, the antenna was elevated by 0.1, 0.5 and 1 mm above the skin. These cases are referred to as Case 2-Case 4, respectively, in Figs. 12-14. Adding the air gap improved the gain significantly, while it did not change the radiation patterns, and the reflection coefficient is still less than -10 dB at the center frequency. However, it caused a significant increase in the resonance frequency, as shown in Table VI. The same procedure was done for antenna above the segmented head model. Please note that for these simulations we had to reduce the mesh size and accuracy due to the size of numerical calculations. The reflection coefficients and gain levels are summarized in Fig. 15 and Table VII, respectively. The results of resonance frequencies are very similar to 4x4 cm^2, while the gain shows some reduction. We conclude that the layered model is a good approximation of full segment model of head when doing quick simulations.

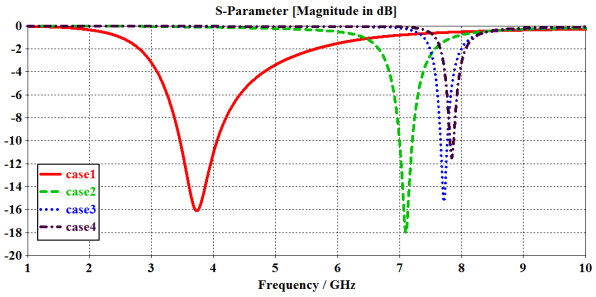

Figure 12. Return loss for cases after adding a dielectric layer, different cases refer to different spacing as listed in Table VI.

TABLE VI. ANTENNA GAIN FOR VARIOUS SPACING ABOVE A 4X4 CM^2 LAYERED MODEL, S IS THE SPACING, F_R IS THE RESONANCE FREQUENCY.

Cases	S (mm)	Gθ (ϕ=0)	Gφ (ϕ=0)	Gθ (ϕ=90)	Gφ (ϕ=90)	f_r (GHz)
1	0.0	-17.9	-134	-38.8	-17.90	3.75
2	0.1	-3.1	-113	-13.2	-3.35	7.10
3	0.5	0.1	-110	-11.0	0.05	7.72
4	1.0	1.4	-109	-11.1	1.36	7.84

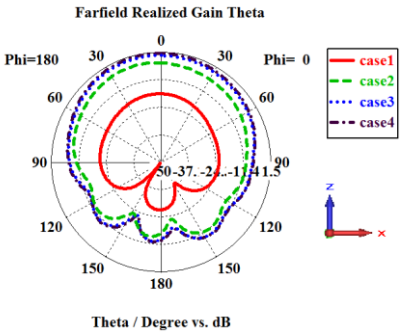

Figure 13. E-plane radiation patterns of cases as listed in Tabel VI.

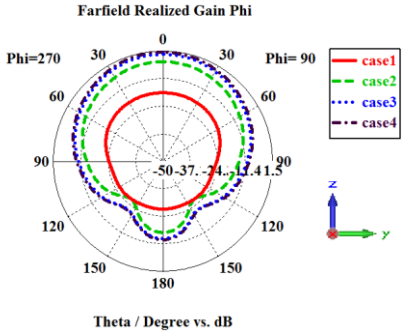

Figure 14. H-plane radiation patterns of cases as listed in Tabel VI.

D. *Specific Absorption Rate*

The Specific Absorption Rate (SAR) is the radiation that is absorbed by the tissue. The maximum SAR limit according to IEEE standards is 1.6 W/kg for 1g of tissue. To comply with this standard, the input power of the antenna, when it is placed 0.5 mm above head, has to be less than 0.257 W. Fig. 16 shows the SAR value after power was reduced.

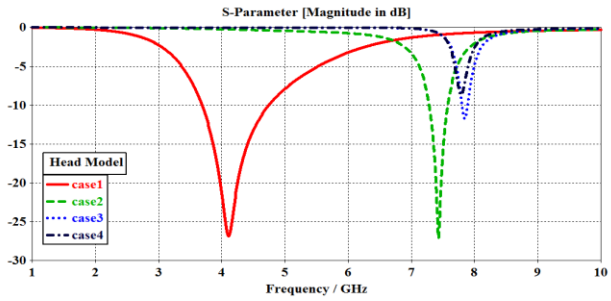

Figure 15. Return loss for cases after adding a dielectric layer, different cases refer to different spacing as listed in Table VII.

TABLE VII. ANTENNA GAIN FOR VARIOUS SPACING ABOVE A HEAD MODEL, S IS THE SPACING, F_R IS THE RESONANCE FREQUENCY.

Cases	S (mm)	Gθ (ϕ=0)	Gφ (ϕ=0)	Gθ (ϕ=90)	Gφ (ϕ=90)	f_r (GHz)
1	0.0	-14.8	-43.0	-32.2	-14.8	4.10
2	0.1	-4.15	-28.4	-16.0	-4.17	7.43
3	0.5	-0.29	-23.2	-9.93	-0.38	7.85
4	1.0	0.36	-23.5	-10.5	0.29	7.79

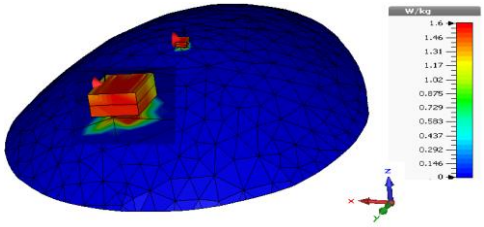

Figure 16. SAR distribution on head model.

IV. CONCLUSION

A miniaturized antenna suitable for integration with sensors is introduced. The antenna is intended to be placed closely to human head. The performance of antenna in the vicinity of human head was modeled and studied. This study showed that there is a trade-off between resonance frequency and gain. For lower frequencies (around 4 GHz) gain will be less than -17 dBi, while by adding a small air gap and shifting the resonance frequency to around 8 GHz, the gain will be increased to more than 0 dBi.

ACKNOWLEDGMENT

The authors would like to thank Mr. Aaron Bergstrom for help in running simulations on cluster computers.

REFERENCES

[1] A. Darwish, and A.E. Hassanien, "Wearable and implantable wireless sensor network solutions for healthcare monitoring," *Sensors*, vol. 11, pp. 5561-5595; doi:10.3390/s110605561, 2011.
[2] https://www.cst.com/Products/CSTMWS, visited March 2014.
[3] M. A. Eleiwa, A. Z. Elsherbeni, "Debye constants for biological tissues from 30 Hz to 20 GHz," *ACES Journal,* vol. 16, no. 3, pp. 202-213, 2001.
[4] http://niremf.ifac.cnr.it/tissprop/ , visited March 2014.
[5] R. Warty, M. Tofighi, U. Kawoos, and A. Rosen, "Characterization of implantable antennas for intracranial pressure monitoring: reflection by and transmission through a scalp phantom," *IEEE Transactions on Microwave Theory and Techniques,* vol. 56, no. 10, pp. 2366-2376, Oct. 2008.